# PREDICTION OF STORE SEPARATION TRAJECTORIES OF THE EGLIN TEST MODEL USING CRADLE CFD

***Ganesh Pawar R[1*], Nuza Nigar[2], Praphul T.[3], Dr. Karthik Sundarraj[4]***

[1]Hexagon Manufacturing Intelligence, Bangalore, Karnataka – 560043, India,
ganesh.pawar@hexagon.com, +91-9916658828
[2]Hexagon Manufacturing Intelligence, Bangalore, Karnataka – 560043, India,
nuza.nigar@hexagon.com, +91-8478929290
[3]Hexagon Manufacturing Intelligence, Bangalore, Karnataka – 560043, India,
praphul.t@hexagon.com, +91-9946231888
[4] Hexagon Manufacturing Intelligence, Bangalore, Karnataka – 560043, India,
karthik.sundarraj@hexagon.com, +91-9900787155

# PREDICTION OF STORE SEPARATION TRAJECTORIES OF THE EGLIN TEST MODEL USING CRADLE CFD


## ABSTRACT

**Testing of store separation involves risk and could result in fatal accidents. It also involves a huge testing cost. The traditional use of flight tests and Wind Tunnel Testing required a very long testing time. With the development in Computational Fluid Dynamics (CFD), it has become easier to simulate there separation. The coupling of Six DOF equations with the Navier Stokes (N-S) equations is needed to establish this. The force and moments on a store can be calculated using CFD applied to the pylon, wing and store geometry. The purpose of this project is to use Software Cradle to validate the store separation trajectory using the Eglin Test Model. This work also presents detailed attention to the ejector force profile. The transonic Mach number for which the simulation is performed is 0.95. The software Cradle's scFLOW code is used to solve the Reynolds Averaged Navier Stokes (RANS) Equation in couple with the 6 Degree of Freedom Equation. The overset meshing technique is employed. The simulation results in good agreement with the Linear and Angular Displacement of the store.**



***Keywords**: Computational Fluid Dynamics, Transonic, Reynolds Averaged Navier Stokes Equation, Store Separation*


## 1. INTRODUCTION

In terms of missile integration, the separation of the store from the air vehicle is critical. During flight at the time of store separation, it is essential that it does not come in contact with the aircraft. [2] Flight tests were traditionally used to test store separation, but they were time-consuming and often required years to certify a projectile.[7] In the 1960s, Wind Tunnel Testing was done to perform the store separation tests. However, such testing had long lead times and limited accuracy. The method used in such a wind tunnel was the Captive Trajectory System. However, the CTS system had no accuracy in time. Thus, they do not account for the inherent unsteadiness encountered by the store during separation. Also, due to the use of small-scale models, scaling problems often lead to a reduction in accuracy.[4] High Parallel Computing and numerical algorithms have paved the way for numerical solutions to Store Separation. Such numerical modelling and simulations have reduced certification costs while increasing flight test safety margins. Recent tests have revealed that the paths of stores released from internal weapons bays deviate from predicted paths. It is critical, in particular, to develop an accurate method of predicting the trajectory of a transonic regime. A complex transient interaction phenomenon exists in a transonic regime, which must be simulated by taking into account the compressibility effects and the strong interference flow fields generated between the pylon, wing, and store body.

**Table 1.** Six Degrees of Liberty Parameters indicating the store mass, the position of the centre of mass, inertial properties, and ejector parameters [8]

| | |
|---|---|
| Mass of the store | 907.185 kg |
| Center of Mass | 1417.3 mm (aft of STV nose) |
| $I_{xx}$ | 27.1163 kg-m2 |
| $I_{yy}$ | 488.0944 kg-m2 |
| $I_{zz}$ | 488.0944 kg-m2 |
| Forward Ejector Force Applied | 10676.01 N |
| Aft Ejector Force Applied | 42703.0 N |
| Forward Ejector Moment | -1920.0 Nm |
| Aft Ejector Moment | 14057.0 Nm |
| Stroke Length of Ejector Piston | 0.10 m |

### 1.1 The Eglin Test Case Model

The Eglin Model consists of the delta wing with NACA 64A010 section of the airfoil with a sweep of 45 degrees. It is followed by a pylon in the shape of an ogive flat plate having an ogive cross-section. The store body which is finned also has the shape of an ogive cylinder with an ogive cross-section. The wing trailing

edge has zero sweep angle and also a taper ratio of value 0.133. The fins are made of a clipped delta wing, four in count and identical having a NACA 0008 section of an airfoil and a sweep angle of 45 degrees. The leading edge sweep angle is 60 degrees and the trailing edge sweep angle is 0 degrees. The distance between the finned body and the pylon is 35.6 mm. The store's length is 3017.5 mm and its diameter is 508.1 mm. Table 1 displays the store mass, position of the center of mass, inertial properties, and ejector parameters. [11] The ejection of the store occurs with a sufficient amount of force in order to maintain a safe separation. It is allowed to fall for 100 mm which is the stroke length of ejection. At this point, the motion of the store is under the influence of aerodynamic and gravitational forces. [3]

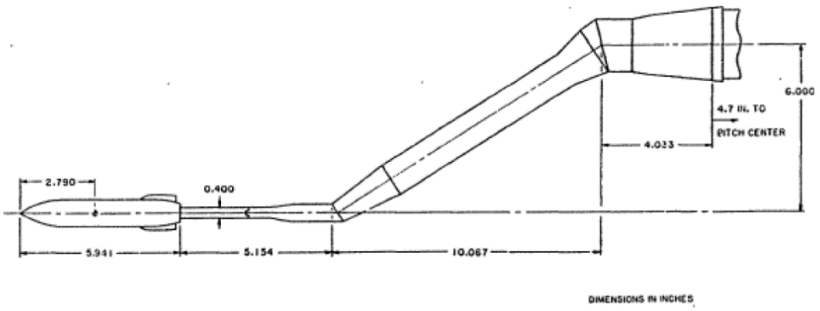


**Figure 1.** Sketch of the Eglin Test Case showing the dimensions in inches [3]

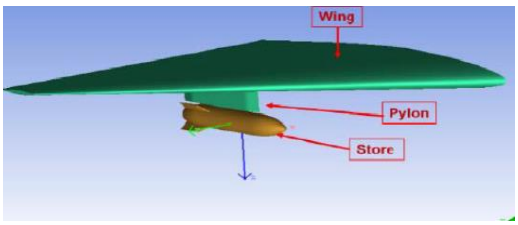


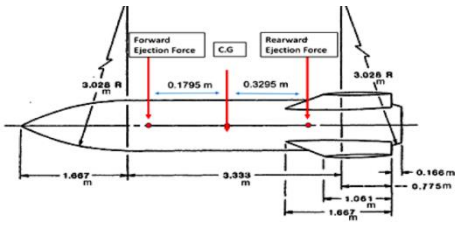


**Figure 2. (left)** Geometry of the wing/pylon/store[10] ; **Figure 3. (right)** Dimensions of The Store[10]

## 2. THE GOVERNING EQUATIONS

### 2.1 Conservation Equations

The N-S relationship describes how pressure, temperature, and density are related to a moving fluid. They are made up of a set of coupled partial differential equations, one for mass conservation, three for momentum conservation, and one for energy conservation, all of which are time-dependent. Although these equations are theoretically possible, they are extremely difficult to solve analytically and are thus more commonly solved on computers using approximations.

Mass Conservation Equation as shown in Equation (1).

$$\frac{\partial \rho}{\partial t} + \frac{\partial}{\partial x_i} \rho u_i = 0 \tag{1}$$

Momentum Conservation Equation as shown in Equation (2).

$$\frac{\partial \rho u_i}{\partial t} + \frac{\partial u_j \rho u_i}{\partial x_j} = \frac{\partial \sigma_{ij}}{\partial x_j} + \rho g_i \tag{2}$$

Energy Conservation Equation as shown in Equation (3)

$$\frac{\partial \rho H}{\partial t} + \frac{\partial u_j \rho H}{\partial x_j} = \frac{\partial p}{\partial t} + \frac{\partial u_j p}{\partial x_j} + \sigma_{ij} \frac{\partial u_i}{\partial x_j} + \frac{\partial}{\partial x_j} K \frac{\partial T}{\partial x_j} + \dot{q} \tag{3}$$

### 2.2 Six Degree of Freedom Equations

scFLOW uses the ALE (Arbitrary Lagrangian-Eulerian) method, which handles both the moving coordinate system and the fixed coordinate system at the same time, to simulate flows around moving objects. In the moving region, the effect of mesh movement is added to the equation of the fixed coordinate system, and the fixed and moving coordinate systems are calculated concurrently. Moving condition setting for a moving region, as well as selection and setting of the connection method for both static and moving regions, are required in the simultaneous calculation with the ALE method. By applying the moving condition to the volume region containing the object, the moving object is represented. Translation and rotation are examples of settable motions. The static and moving regions can be connected by an overset mesh.[6]

The effects of element motions are incorporated into the equations for the fixed coordinate system in ALE. The following effects are added to the fixed coordinate system's mass conservation equation and momentum equations [9]

Equation (4) shows the Mass Conservation Equation in Fixed Coordinate System.

$$\frac{\partial \rho}{\partial t} + \frac{\partial}{\partial x_i}\rho(u_i - v_i) = 0 \tag{4}$$

Equation (5) shows the Momentum Conservation Equation in Fixed Coordinate System.

$$\frac{\partial \rho u_i}{\partial t} + \frac{\partial (u_j - v_j)\rho u_i}{\partial x_j} = \frac{\partial \sigma_{ij}}{\partial x_j} + \rho g_i \tag{5}$$

In the energy conservation (the second term on the left side of the equation) must be replaced by $(u_j - v_j)$. The term $v_j$ refers to the mesh's speed of movement.

The complex movement of the object under investigation is simulated using the Six DOF Motion for the combination of the moving elements. The equation of motion can be used to calculate fluid pressure and viscous stress, as well as the motion of a rigid body subjected to an external force. The mass and moment of inertia of the portion moving as the rigid body are automatically calculated from its material properties to construct the equation of motion. Using the object's forces and moments, the Six DOF solver computes the translational and angular motion of an object's centre of gravity. The governing equation for the translational motion of the centre of gravity is solved in the inertial coordinate system.

$$\dot{\vec{v}}_G = \frac{1}{m}\sum \vec{f_G} \tag{6}$$

$\dot{\vec{v}}_G$ is the translational motion of the center of gravity, m is the mass, and $\vec{f_G}$ is the gravitational force vector. Using body coordinates, the angular motion of the object, $\dot{\vec{\omega}}_B$, is more easily computed as shown in Equation (7).

$$\dot{\vec{\omega}}_B = L^{-1}\left(\sum \vec{M}_B - \vec{\omega}_B \times L\vec{\omega}_B\right) \tag{7}$$

Here, where $L$ is the inertia tensor, $\vec{M}_B$ is the moment vector of the body, and $\vec{\omega}_B$ is the rigid body angular velocity vector. The moments are transformed from inertial to body coordinates using Equation (8).

$$\vec{M}_B = R\vec{M}_G \tag{8}$$

As a result, the translational equation uses three translational degrees of freedom to describe the aircraft, whereas the rotational equation uses three rotational degrees of freedom. As a result, Newton's second law yields six equations for the six degrees of freedom of a rigid body. Two sets of equations must be solved concurrently to predict the trajectory of store separation: Navier-Stokes equations and Equations of motion.

## 3. CFD Modelling and Simulation

### 3.1 CAD Modelling

The Eglin Test Model, which includes the pylon, wing, and store, is modeled, and an external flow domain, known as the computational domain, is added to analyse the external flow over the model. The computational

domain must be large enough so that it has no effect on future computations.A cylindrical domain is created on the store which is used to create overset mesh over the domain. The two meshing units of the overset mesh that are created in scFLOW are the background unit and the component unit. The background unit consists of the wing and the pylon, whereas the component unit consists of the missile body.

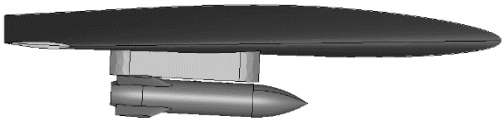

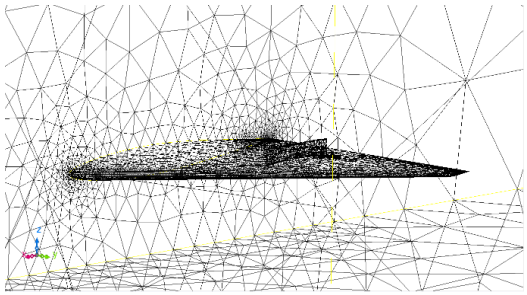

**Figure 4. (left)** The Eglin Model Geometry created in scFLOW; **Figure 5. (right)** Build Analysis Model showing tiny facet creation on the model.

scFLOW has the feature of building the analysis model out of the CAD. By doing this, several facets are created on the model which helps in removing all the unnecessary curved edges that may interfere with the solution. Since there are two components of the overset mesh that consist of the geometry, the build analysis model will be created twice, one for each unit. This group of triangle facets which are created during the build analysis model is used for subsequent mesh generation.

### 3.2 Material Specification and Analysis Conditions

The wing pylon body and the missile body are modeled as an obstacle. The fluid around the obstacle is modeled as the compressible air at 20 degrees Celsius.

The density-based solver is used because the flow in the study is compressible. The density-based solver solves simultaneous equations without first converting them to conservation equations. Mass conservation solves the mass conservation problem for compressible fluids by tracking the density change rigorously. Due to the interdependence of density, pressure, temperature, and velocity, the system of equations can be closed by adding an equation of state to each conservation equation. The standard k-EPS turbulence model was used in this study. [12] The k-EPS model is a two-equation closure model with two additional transport equations, Turbulence Kinetic Energy k and Turbulence Dissipation Epsilon

**Table 2.** Flow Analysis Conditions used in the study.

| **Parameters** | **Value** |
|---|---|
| Mach Number | 0.95 |
| Static temperature | 236.7 K |
| Reference Pressure | 36042 Pa |
| Mach No. | 0.95 |
| Turbulence model | RANS, k-epsilon |
| Time-step | 1e-04 [s] |
| No. of elements | 2.2 million |

The steady-state calculation is performed without the use of Six DOF Equations in the early stages of the simulation. The steady-state simulation results are used as the initialization for the transient state calculation. The steady-state simulation was run for 2000 cycles for this study. The temperature is set to 236.7 K by default. As the model's orientation, gravity is considered in the positive Z direction, and the base value of pressure is specified as equal to the absolute pressure. The time-step for the transient analysis is set to 0.0001 as well as

the simulation is run for 0.32 seconds. [11] The simulation was run in the transonic regime. The Mach number in question is 0.95. [11] The velocity component and the Mach number are specified at the inlet. As the inlet is registered in the same direction, the velocity component is in the negative X direction. The outlet is defined as the Static Pressure (Outflow), with a pressure value of 36042 Pa. The 'free slip' wall boundary condition is defined by the top, bottom, and ymax.

### 3.3 Coupling using Six Degrees of Freedom

The computations start at t = 0s to obtain the aerodynamic forces and moments, and the solver is then coupled with a 6-DOF code to predict the entire store trajectory using the quasi-steady approach. Both forward and aft ejector forces are applied to the store, which are turned off once the ejector stroke lengths are exceeded. The expected outcome of applying these ejector forces is that the store pitches up for a real-time of t = 0.06 seconds due to ejector forces acting on it. After the ejector forces have worn off, aerodynamic forces acting on the store take control, resulting in a pitch-down moment. [5] Table 1 displays the six DOF parameters. The forward and the rearward ejector force is applied in the tabular format according to their working since the ejector forces act for 0.06 s and then stop.

### 3.4 Analysis Control Methods

To set the under-relaxation coefficient, for the system of equations of the density-based solver, a 0.2 value has been specified. The under-relaxation coefficient for the equations of density-based solver and turbulence and diffusion is set as 0.2,0.7 and 0.99 respectively. Second-order accuracy with a limiter is used for the Accuracy of the convective terms for the mass, momentum, energy, turbulence, and diffusion equation. First Order Accuracy of Time Derivative is used. The Least Square Method is used for Gradient Calculation.

### 3.5 Mesh

Elements are placed in a region to analyze physical phenomena and calculate changes in physical quantity. scFLOW includes a polyhedral mesher (arbitrary polyhedrons) to improve the cell-centered Solver's stability and calculation accuracy. This is an automatic mesher that will generate mesh based on the number of elements specified, making mesh fine near the wall surface where a rapid flow change is anticipated. The mesh generation involves the creation of an octree and the generation of the polyhedral mesh along with the prism layers which are inserted along the wall.

Due to the use of the overset mesh, the octree creation also takes place separately for each of these units. For the first meshing unit, the minimum octant size for all the surfaces is given as 12.8 and the maximum octant size is also of the same value. Since there is space in the far field, octants are coarsened up to this size, which is the maximum octant size. The octant refinement level is specified from the near wall up to the far field. For the second meshing unit, the minimum and the maximum octant size are specified as 0.1, for the same reasons stated above. The number of elements generated for meshing units 1 and 2, while creating the octree is 2,254,965 and 280,709 respectively.

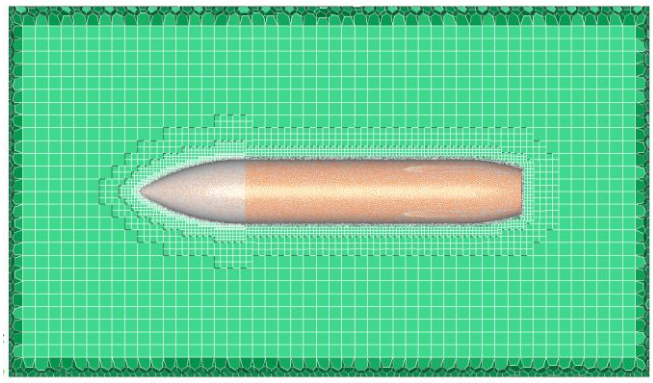

**Figure 6.** Meshed missile body showing prism layer along the walls and polyhedral (unstructured) mesh generation.

scFLOW automatically provides the creation of the prism layer along the walls. Since The distance from the wall is not uniform without the prism elements, sufficient accuracy cannot be obtained for velocity and temperature gradient. However, with the prism elements, the distance from the wall becomes uniform. Sufficient accuracy can be obtained for velocity and temperature gradient as well as the prism layer has the advantage of both calculation accuracy and stability. Here the prism layer is generated along the walls of the wing, the pylon, and the store. The number of prism layers specified here is 2 and the thickness of the prism

layer is 0.2. As the polyhedral which is an unstructured mesh is generated, the final count of the number of elements is 2,201,265.

# 4. ANALYSIS RESULTS

## 4.1 Linear Displacement versus Time Graph

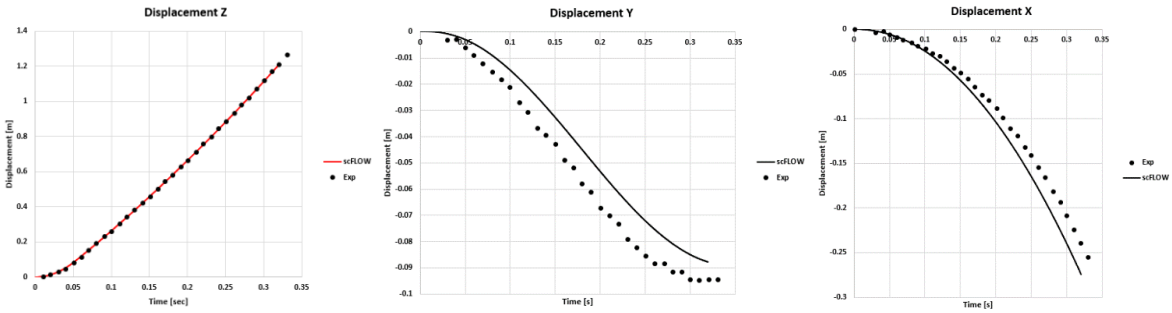


**Figure 7(a-c).** Linear Displacement versus Time graph in X, Y, and Z direction comparing the numerical and the experimental data.

The store separation begins when the ejector forces act. The ejector forces are applied to the store during ejection initiation. When gravity and ejector forces separate the store from the aircraft, it begins to move backward, downward, and inward. The inward and backward movements begin around t=0.2 seconds, as shown in Figure 9.

Figure 7(a-c) depicts the store's X, Y, and Z translations. The experimental data for the rigid wing appear to closely match the Z translation. There was a minor difference between the X and Y trajectories. This is due to the fact that in the Z direction, the ejector and gravity forces outweigh the aerodynamic forces. Because drag is understated due to viscous effects, the small difference in horizontal displacement is to be expected.

## 4.2 Angular Displacement versus Time Graph

Figure 8(a-c) compares the experimental and numerical store trajectory for the center of gravity angular orientations with respect to time. Because of the dominance of aerodynamic forces, the store moves in a pitch-up, negative yaw, and positive roll direction.

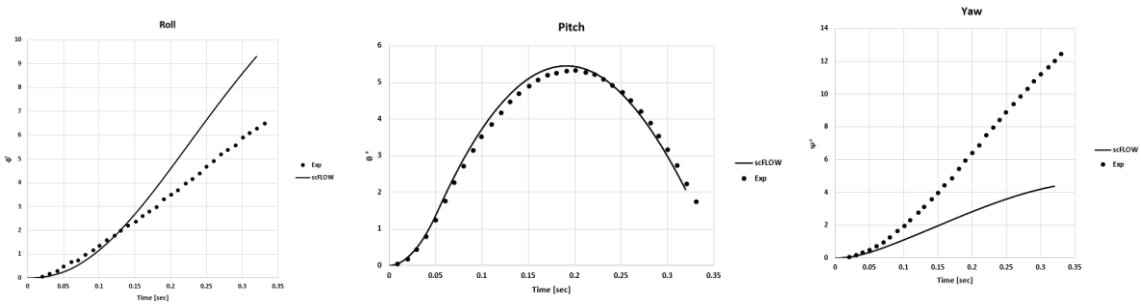


**Figure 8(a-c).** Roll, Pitch, and Yaw versus time graph comparing the numerical and the experimental data.

In Figure 8(a), the numerical roll trend shows a similar trend to the experimental data. Although the trend is very similar, the results show a minor deviation from the experimental data. This deviation is seen after 0.05 second which is when the ejector forces also disappear.

The pitching trend in Figure 8(b) is very close to the experimental data. Because aerodynamic and ejection forces exist, the store initially moves in a pitch up direction. When the ejector forces are removed, the store's motion results in a pitch down movement.

In Figure 8(c), the yaw orientation shows a similarity in trend when compared to the experimental data. Minor deviations occur near time 0.30 seconds.

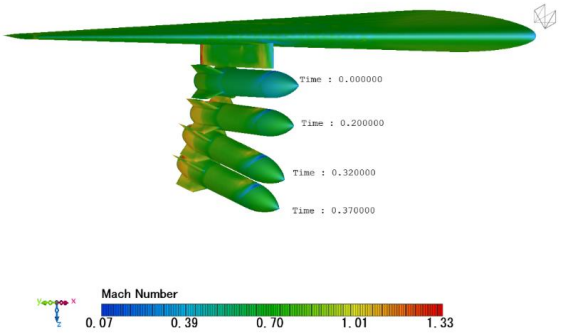


**Figure 9.** The Store Separation with Event Ejectors at Mach 0.95

## 5. CONCLUSION

The study performed using the Eglin Test Model at Transonic Mach Number using scFLOW successfully predicts the influence of ejector and gravity forces on the store trajectory which overcomes the aerodynamic force. The linear displacement in the z direction matches very well with the experimental data. Also, the pitch orientation shows a good agreement. The ease of use of Overset Mesh in scFLOW enables the ease of application of the Six DOF feature for coupling with the Navier – Stokes Equation. Software Cradle provides a very comprehensive way of post-processing that enables easy analysis of results.

## ACKNOWLEDGMENT

A token of gratitude to Dr. Rajesh Yadav, Assistant Professor, University of Petroleum and Energy Studies for his support. Also, would like to thank Hexagon Manufacturing Intelligence, India for providing this opportunity to conduct the study.

## REFERENCES

[1] Arbitrary Lagrangian-Eulerian Method. (n.d.). Retrieved May 9, 2022, from http://www.me.sc.edu/research/jzuo/Contents/ALE/ALE_1.htm

[2] Demir, H. Ö., Selimhocaoğlu, B. T., & Alemdaroğlu, N. (n.d.). CFD Applications in Store Separation Görkem DEMİR.

[3] E. HEIM, "CFD Wing/Pylon/Finned Store Mutual Interference Wind Tunnel Experiment", Arnold Engineering Development Center, AD-B152 669, September 10-17, 1990

[4] Madasamy S, Thilagapathy G, & Arulalagan R. (2016). Investigation of Store Separation and Trajectory of Weapons in Military Aircraft. International Journal of Scientific & Engineering Research, 7(2). http://www.ijser.org

[5] Osman, A. A., Bayoumy Aly, A. M., El, I., Abdellatif, O. E., & Khallil, E. E. (n.d.). Investigation of the Effect of Grid Size on External Store Separation Trajectory using CFD.

[6] Overset Mesh - Fluid Codes - Ansys Engineering Simulation. (n.d.). Retrieved May 9, 2022, from https://fluidcodes.com/software/overset-mesh/

[7] Panagiotopoulos, E. E., & Kyparissis, S. D. (n.d.). CFD Transonic Store Separation Trajectory Predictions with Comparison to Wind Tunnel Investigations.

[8] Riboli, F. M. (n.d.). Store Separation Predictions for Weapon Integration on a Fighter-Type Aircraft Safe Separation Simulation View project. https://www.researchgate.net/publication/346714232

[9] scFLOW User's Guide Analysis Method - 04/Nov/2021. (n.d.).

[10] Sheharyar, M., Uddin, E., Ali, Z., Zaheer, Q., & Mubashar, A. (2018). Simulation of a standard store separated from a generic wing. Journal of Applied Fluid Mechanics, 11(6), 1579–1589. https://doi.org/10.29252/jafm.11.06.28865

[11] Sunay, Y. E., Gülay, E., & Akgül, A. (2013). Numerical Simulations of Store SeparationTrajectories Using the EGLIN Test. In Scientific Technical Review (Vol. 63, Issue 1).

[12] Versteeg, H. K., & Malalasekera, W. (1996). An introduction to computational fluid dynamics: the finite volume method, 1995. Harlow-Longman Scientific & Technical, London, M, 503.